BACHELOR

Quantifying specific aggregation rates of PSA-antibody coated particles using an optomagnetic cluster experiment

Coers, J.M.

Award date:
2019

Eindhoven University of Technology

Molecular Biosensing for Medical diagnostics (MBX)

Bachelor Final Project

Quantifying specific aggregation rates of PSA-antibody coated particles using an optomagnetic cluster experiment

J.M. Coers (0904471)

supervised by M.R.W. Scheepers and L.J. van IJzendoorn

Date: 31/10/2019

Abstract

With the use of an optomagnetic cluster (OMC) experiment we were able to measure specific aggregation rate for particles coated with antibodies against prostate specific antigen (PSA). Initially, we investigated superparamagnetic particles (500nm) made by Ademtech and MicroParticles GmbH for their use in the OMC experiment. Additionally, three common aggregation suppressors – bovine serum albumin (BSA), Pluronic F-127 and Tween 20 – were tested to suppress non-specific particle aggregation. We found that Ademtech polystyrene particles were most suitable for this experiment in combination with BSA.

In order to measure the non-specific aggregation rate in the presence of PSA an experiment was conducted with particles covered with the same type of antibody. In this experiment no increase in aggregation rate was observed with increasing PSA concentration.

To induce specific binding, the particles were coated with both types of antibodies and measurements showed that the aggregation rate increases with increasing PSA concentration up to a certain point where the binding sites on the particle get saturated and the aggregation rate decreases. In the measurements the upper limit of the experimental setup was reached. By lowering the antibody surface concentration on the beads the aggregation rate could be tuned and was decreased to below the limit.

Table of Contents

1. Introduction

Nano- and microparticles are used in a wide variety of biomedical applications, e.g. biosensing [1], drug delivery [2] and magnetic resonance imaging [3]. They can be produced and customized, in material, size and shape, to meet the requirements of the application. One example is the detection of biomarkers using an optomagnetic cluster assay in point of care sensing where fast and accurate diagnosis is desired. In this application superparamagnetic particles are used to accelerate cluster formation [4] and increase detection accuracy [5].

Ranzoni et al. showed that an optomagnetic cluster assay can be used to measure prostate specific antigen (PSA) concentrations [5]. PSA molecules are captured by antibodies coated on microparticles. When a particle that has captured an analyte molecule encounters another particle by diffusion they can form a dimer. By using superparamagnetic particles in combination with an external magnetic field the encounter rate is accelerated due to magnetic dipole-dipole interaction between the particles. After particle aggregation reaches equilibrium, the total amount of dimers is determined by rotating the magnetic field and measuring the oscillation in scattered light. Ranzoni et al. were able to measure PSA concentrations in sub-picomolar range.

Stijn Haenen has previously measured specific aggregation rates for a model system of particles coated with DNA docking strands and a complementary DNA analyte. Specific particle aggregation rates have not yet been measured for an immunoassay. Measuring a particle aggregation rate by using the OMC experiment for PSA coated antibodies is the goal of this project.

We first investigate how to suppress non-specific particle aggregation by varying particle type and adding aggregation suppressors. We then look at the non-specific particle aggregation in presence of PSA molecules by only using one type of antibody so no two particles can capture the same PSA molecule. Finally we look at the specific particle aggregation rate with varying concentrations of PSA molecules.

2. Experimental concept of model assay

In this project we will study the aggregation rate of particles in the context of their use for biomarker detection. Previously, Stijn Haenen has used a DNA model system consisting of particles coated with DNA docking strands in combination with DNA analyte strands to study specific particle aggregation [6]. Here, we will use particles coated with antibodies together with prostate specific antigen (PSA) to induce specific particle aggregation. These clusters can be detected with an optomagnetic cluster (OMC) experiment. In this section the concepts of this experiment will be explained.

2.1 Antibody sandwich system

In order to study particle aggregation an antibody sandwich system is used, see Fig. 2.1. Particles are coated with PSA antibodies such that in the presence of PSA molecules specific molecular bonds can form between particles. Antibodies bind to antigen molecules through a key-lock mechanism, i.e. multiple weak noncovalent bonds between the paratope on the antibody and the epitope on the antigen that geometrically fit onto each other, creating a single stable bond. For monoclonal antibodies, the paratope of the PSA antibody has a high affinity only for its corresponding epitope on the PSA molecule. We use a matched pair of antibodies that target two different epitopes on the PSA molecule to enable binding to a PSA molecule by two antibodies at the same time, without sterically hindering each other. The typical thermal dissociation time of a monoclonal antibody-antigen bond is in the order of 10^5 s [7], which is longer than the five minute measurement time. This implies that the formation of a single bond between two particles will be stable enough to be detected.

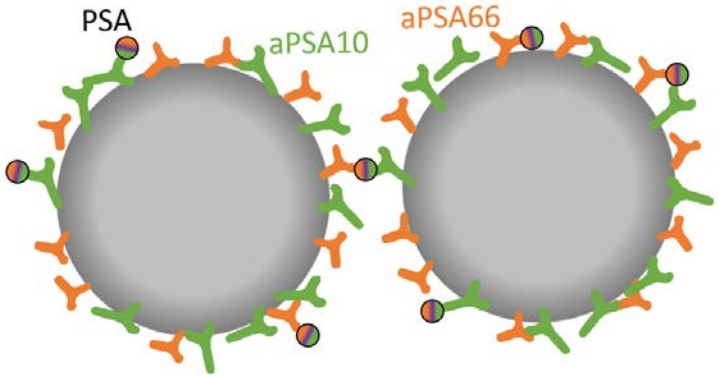

Fig. 2.1. Schematic representation of a dimer in the antibody sandwich system. *Particles are covered with aPSA10 and aPSA66 antibodies. Each antibody binds only to one specific epitope on the PSA molecule.*

2.2 Particle dimer formation rates

Dimer formation, the onset of particle aggregation, is a multistep process. Fig. 2.2 shows this process for two cases, with and without an attractive interparticle force.

For a system without interparticle forces, the first step is for the particles to encounter due to Brownian motion and form an encounter complex. The rate at which this occurs is k_{enc}^{th}. After an encounter complex is formed, there are two possibilities. Either the particles form a chemical bond, this can be anything from a covalent bond, a hydrophobic bond or in our case, the bond between an antibody and antigen. When the particles are chemically bound, they are considered a chemical dimer. The rate associated with this step is the thermally induced chemical aggregation rate, k_{agg}^{th}. If the two particles do not form a chemical bond, they will separate again. The separation rate is k_{sep}^{th}. For colloidal systems that are stable over a long time $k_{sep}^{th} \gg k_{agg}^{th}$.

For the system with interparticle force, in this project a magnetic force, the encounter step is accelerated because of the superparamagnetic properties of the particles (see section 2.3). The dipole-dipole interaction between particles results in an attractive force between particles along the direction of the magnetic field lines. This results in a larger encounter rate. When two particles encounter, they form magnetic dimers at a rate given by k_{enc}^{mag}. Because the magnetic potential is higher than the thermal energy, the particles do not separate anymore, $k_{sep}^{mag} = 0$ (see section 2.3).

Chemical aggregation can be induced by a number of interactions. In this project we distinguish between specific interactions, the antibody-antigen binding, and nonspecific interactions, which include all other bonds, for example Van der Waals- and ionic interactions. In experiments, both specific and nonspecific interactions are present at the same time, so the aggregation rate is a sum of the specific aggregation rate and the nonspecific aggregation rate, see eqn 1.

$$k_{agg}^{mag} = k_{agg,sp}^{mag} + k_{agg,non-sp}^{mag} \quad (1)$$

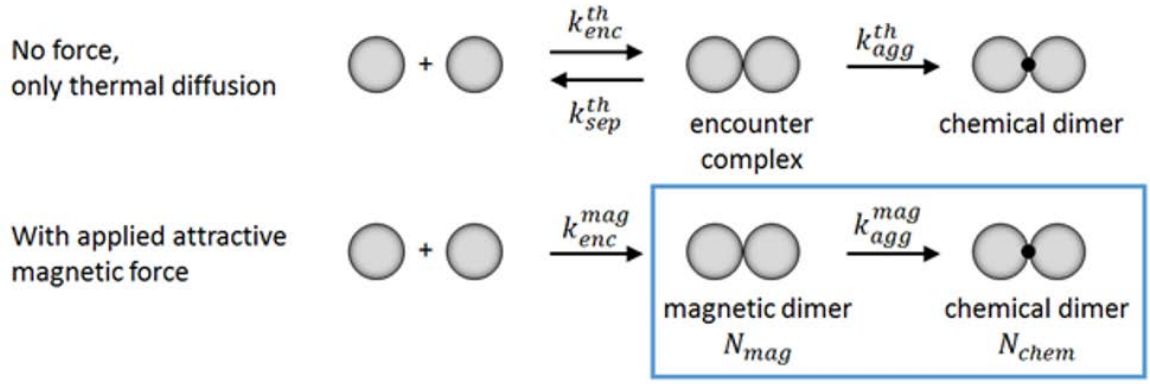

Fig. 2.2. Schematic of rates associated with dimer formation. *Multistep process of chemical dimer formation for both thermally and magnetically induced aggregation. For thermal aggregation, the particles encounter and separate following Brownian motion. In the case that the particles in an encounter complex engage in a chemical bond they form a thermally induced chemical dimer. For superparamagnetic particles in a magnetic field, the particles attract each other due to the induced dipole interaction and form a magnetic dimer. The energy associated with this attraction is much larger than the thermal energy so the particles do not separate. Particles in a magnetic dimer can engage in a chemical bond to form a magnetically induced chemical dimer.*

2.3 Superparamagnetic particles and magnetic interactions

In this project we use superparamagnetic particles to induce an attractive interparticle force. These superparamagnetic particles consist of many ferromagnetic grains embedded in a nonmagnetic matrix. The grains consist of a single domain, having a well-defined magnetization in random direction at each point in time. The direction of magnetization flips in a typical time called the Néel relaxation time, which is dependent on the size of the grain and their magnetic crystal anisotropy [8]. In absence of an external magnetic field, relatively small grains flip direction many times per second while larger grains will flip much slower. Because the direction of magnetization is random for all grains, the net magnetic moment of a particle is zero. In the presence of an external magnetic field, the magnetization of a grain will stay in the direction parallel to the magnetic field a larger fraction of the time. This results in a net non-zero magnetic moment of the particle in the direction of the applied magnetic field.

In an external magnetic field, two paramagnetic particles will attract each other due to the dipole-dipole interaction. Assuming the particles as parallel point dipoles, the potential at an interparticle distance d_0 for this interaction is given by eqn. 2

$$U_{mag} = \frac{\mu_0 m_1 m_2}{2\pi d_0^3} \quad (2)$$

where μ_0 is the vacuum permittivity and m_1 and m_2 are the magnetic moments of the dipoles. For the parameters used in this project (X_v = 2, R = 256nm, B = 4mT), at a distance of 0.5μm where the particles come in contact, $U_{mag} \approx -80\mathrm{k_B T}$. This is much larger than the thermal energy at room temperature. Two particles that encounter while under the influence of an external magnetic field are called a magnetic dimer. Because the potential energy is large compared to the thermal energy, magnetic dimers will not separate.

When the magnetic field is turned off, the magnetic moments of ferromagnetic grains go back in random orientation and the particles will lose their net magnetic moment. Note that particles in a magnetic dimer that don't have any other bonds between them will drift apart due to Brownian motion. Particles that do have a bond between them will stay together and are called a chemical dimer.

3 Materials and Methods

In this chapter we will discuss the materials and the methods used in this project. The functionalization of particles will be explained as well as the optomagnetic clustering experiment.

3.1 Materials

Carboxylated superparamagnetic Masterbeads were purchased from Ademtech (diameter 0.5 µm, coefficient of variation 25%). Carboxylated superparamagnetic silica particles were purchased from Microparticles GmbH (diameter 0.5 µm, coefficient of variation 6%). α-PSA10 and α-PSA66 monoclonal antibodies were obtained from Fujirebio. PSA antigen was purchased from HyTest. PBS tablets, MES, EDC, NHS and Tris were purchased from Sigma Aldrich as well as Pluronic f-127, Tween-20 and Bovine Serum Albumin (BSA). The sonic finger is obtained from Hielscher. Borosilicate glass cuvettes with square cross section (inner dimension 1.00 ± 0.05 mm, outer dimension 1.23 ± 0.05 mm, length 20 ± 1 mm) were purchased from Hilgenberg. The laser (Mode Hitachi HL6545MG laser) with a wavelength of 660 nm, lenses and photodetector (PDA36A-EC Si amplified detector) are purchased from Thorlabs. Interface card (NI USB-6211) is obtained from National Instruments.

3.2 Particle functionalization with PSA antibodies

In order to study the aggregation rate of particles via the interaction of PSA and α-PSA antibodies, the particles need to be functionalized. In this section the protocol for functionalization is described.

4µL of carboxylic acid coated particles are suspended in 196µL MES buffer (100mM MES, pH 5.0) to a particle concentration of 10pM. The suspension is sonicated (10 pulses of 0.5s at 50% power) to break as many present clusters as possible. 50µL of EDC (10 mg/mL in MES buffer) is added to the particles as well as 50µL of NHS (10 mg/mL in MES buffer). During 60 minutes of incubation the COOH groups of the particles get activated. EDC binds to the COOH groups on the particles and subsequently gets replaced by the NHS group. The activated sites on the particles can bind with NH2 groups on antibodies. After the incubation the particles are magnetically washed to remove excess EDC and NHS from the solution. The particles are resuspended in MES buffer, followed by sonification (10 pulses of 0.5s at 50% power). Antibody stock solutions are diluted with MES buffer to 0.09mg/mL. 25 µL of α-PSA10 and 25 µL of α-PSA66 solution is added to the particles, corresponding to 6000 antibodies per particle. This amount is calculated to saturate a particle with antibodies if they are laying flat on the surface assuming perfectly spherical particles with a surface area of $7.8*10^5$ nm^2 and antibodies with dimensions 15x9x4 nm. The antibodies are incubated for 120 minutes. Subsequently, 100µL of TBS buffer (100mM NaCl, 50mM tris, pH 7.6) is added to block residual NHS groups on the particle surface. After an overnight incubation the particle solution is magnetically washed to remove unbound antibodies and excess TBS. The particles are resuspended in 400µL PBS and sonicated (10 pulses of 0.5s at 50% power).

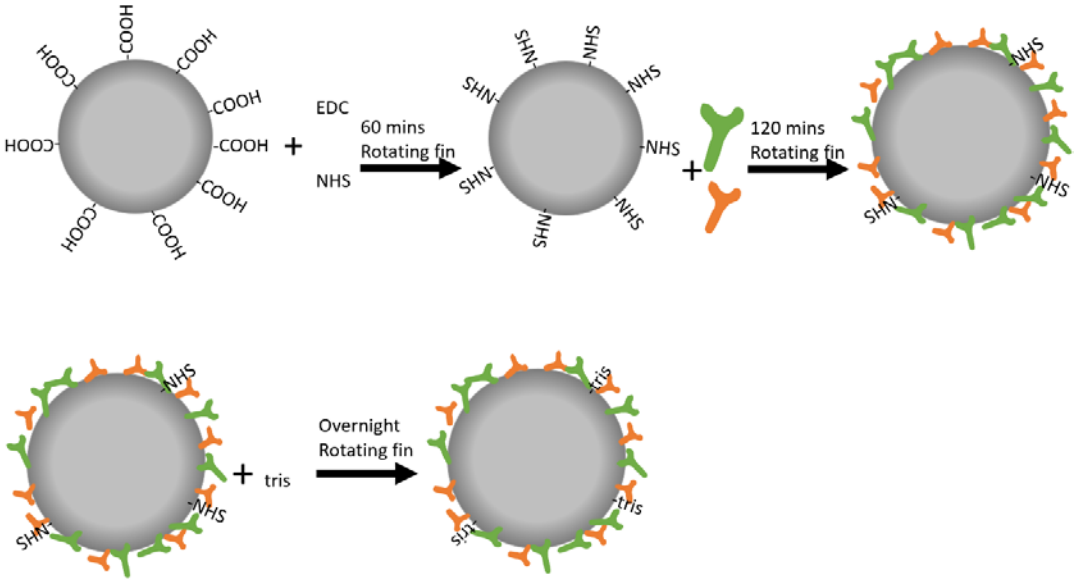

Fig 3.1. Schematic view of particle functionalization. *Particles coated with carboxyl groups get activated by addition of EDC and NHS. After activation, primary amine groups on antibodies can bind on the activated sites. Remaining active sites get blocked by tris molecules to stabilize them.*

3.3 Optomagnetic cluster (OMC) experiment

In this project we use the optomagnetic cluster experiment to measure particle aggregation rates. Magnetic fields are used to accelerate particle aggregation of superparamagnetic particles and we use scattering of light in combination with rotation of the magnetic field to determine the dimer concentration. In this section the experimental setup and its components are described as well as the analysis method of the obtained signal.

3.3.1 Experimental setup

In this section the components and setup of the experiment are described in detail. In Fig. 3.2 a schematic top-view of the setup of the optomagnetic cluster experiment can be seen. A 660nm laser (1) emits an elliptic beam that is made circular using two cylindrical lenses. The beam is then focussed through a 20µm pinhole to simulate a point source. A final lens (f = 150mm) focusses the beam on the cuvette (2) containing the particle solution. The cuvette is surrounded by four electromagnets (3). The currents in the electromagnets are controlled by an interface card that is controlled by a Labview program. (5). In order to create a rotating magnetic field an oscillating current is sent through the electromagnets with a phase difference of 90° between neighbouring magnets. This creates a rotating magnetic field that is uniform within the boundaries of the observation volume. Due to the applied rotating field, the dimers rotate in the cuvette and induce an oscillating intensity of the scattered laser light in the detector (4), which is situated at 90° with respect to the incoming laser beam. The signal of the photodetector is converted to a digital signal using the NI interface card and analysed by the computer.

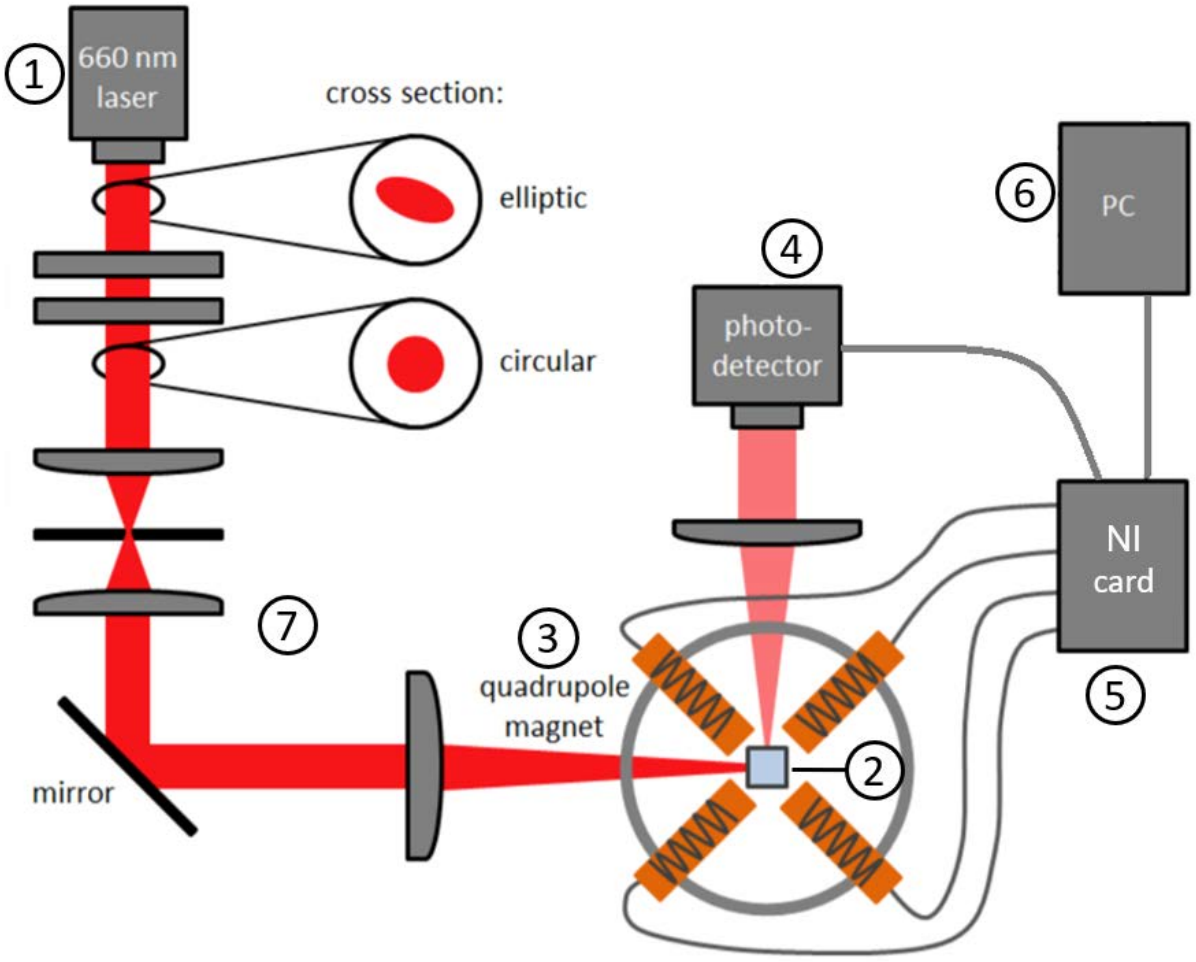

Fig. 3.2 Experimental setup: *Schematic representation of the experimental setup used to measure particle aggregation. 1. Laser that emits elliptical laser light. 2. Cuvette with particle solution. 3. Quadrupole electromagnet that creates a rotating magnetic field. 4. Photodetector that collects light scattered from the cuvette. 5. National Instruments interface card that converts instructions from a Labview program to a voltage which is send to a voltage regulated current amplifier for the electromagnets. The card also converts the analog signal from the photodetector to a digital signal that gets sent to the PC. 6. Computer that runs the Labview program and collects the photodetector data. 7. Optical train that consist of two cylindrical lenses to convert elliptical beam to circular beam, lenses that focus the beam through a pinhole to create a point source and a lens that focusses the beam onto the cuvette.*

3.3.2 Signal analysis

To study the amount of clusters in the system we need to analyze the scattering signal of the photodetector. An example of such signal is given in Fig. 3.3a. The voltage output of the detector oscillates over time with the rotation of the dimers. The characteristics of the signal is dependent on several factors like amount of particles, variation in particle size and interparticle distance. Determining all the factors and characteristics is beyond the scope of this project. Roland van Vliembergen has done extensive research on this topic [9]. The amplitude of the oscillating signal is dependent on the amount of dimers. Monomers do not give a contribution in the oscillation because of their rotational symmetry. A Fourier analysis is applied to the oscillating signal and multiple frequency components can be discerned. This can be seen in Fig. 3.3b. The peaks of the Fourier amplitudes are at frequencies that are multiples of two times the rotational frequency of the magnetic field because of the two-fold rotational symmetry of dimers. In this project we use the amplitude of the 4F peak to determine

the amount of dimers in the solution because it scales linearly with the amount of dimers in the solution.

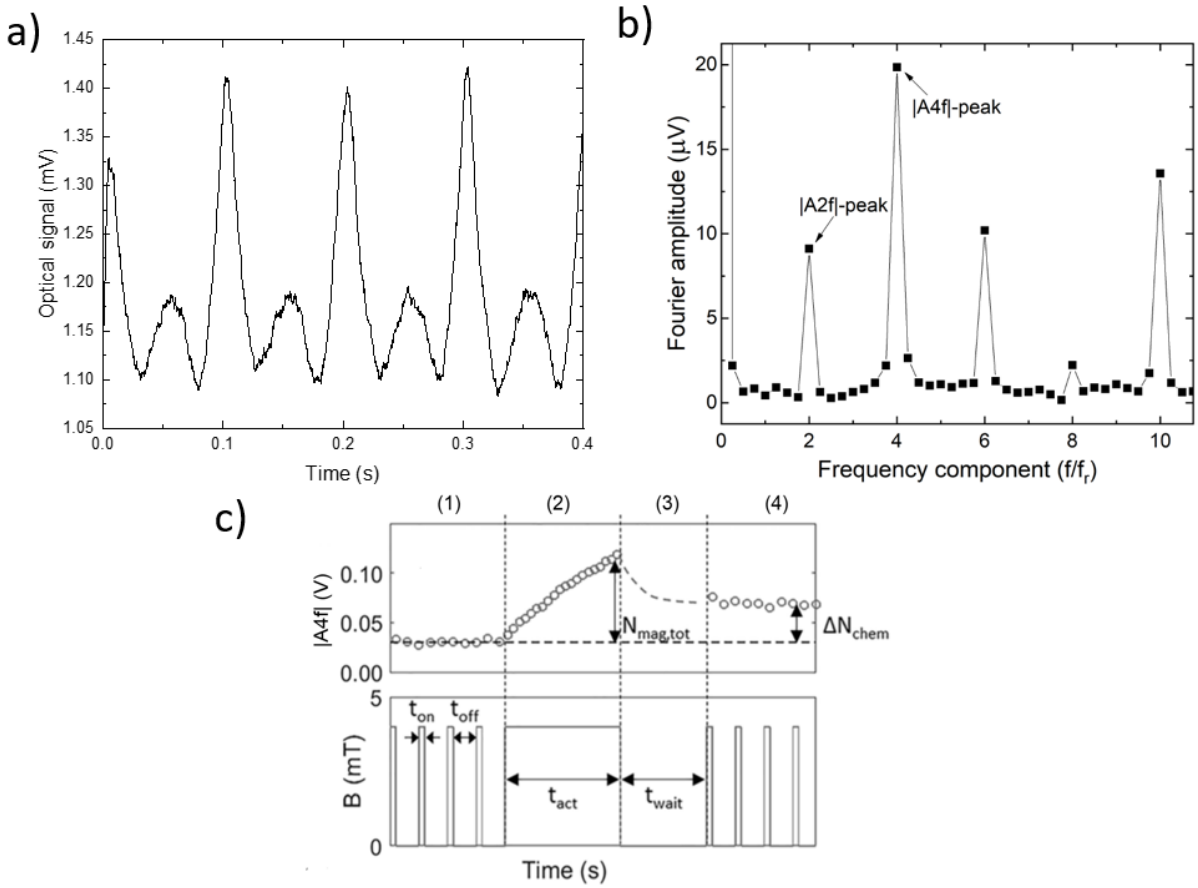

Fig. 3.3 Analysis and protocol of Optomagnetic clustering experiment: *a) Signal voltage of the photodetector. b) Fourier analysis of the photodetector signal. c) Four step protocol to quantify the aggregation rate. (1) Short magnetic pulses that serve as measurements to determine the initial amount of dimers. (2) Actuation phase. Long pulse to encourage magnetically induced particle aggregation. (3) Waiting phase to allow particles to disperse if they did not form a chemical bond. (4) Measurement phase of short pulses to determine the number of formed dimers.*

3.3.3 Quantifying the aggregation rate k_{agg}^{mag}

To measure the aggregation rate of the particles, k_{agg}^{mag}, we use a four step protocol developed by Scheepers et al. [6]. The protocol can be seen in Fig. 3.3c.

The first step of the protocol is to measure the initial amount of dimers with short magnetic pulses, t_{on} = 0.4 s. These pulses are long enough for the chemical dimers to make two full rotations but short enough that little to no additional magnetic dimers form due to interparticle attraction. After each pulse there is a waiting time, t_{off} = 10 s, to give particles enough time to redisperse. Ten measurement pulses are done and the mean of the |A4f| peak is calculated.

After the initial measurement, an actuation pulse is applied to form magnetic clusters, t_{act} = 20 s. Because of the superparamagnetic properties of the particles they attract each other to form magnetic dimers. The total number of magnetic dimers formed during the actuation phase is denoted with $N_{mag,tot}$. The third phase of the measurement protocol is a waiting phase, t_{wait} = 40 s, where the magnetic dimers are allowed to redisperse. The magnetic dimers that made a chemical bond during the actuation phase will stay together. The last step is a measurement

step, similar to step 1, to measure the final amount of chemical dimers. The difference between the initial amount of dimers and the final amount is ΔN_{chem}.

During the actuation phase, when the particles are magnetic dimers, the particles are in close contact for a extended period. During this period a fraction of the magnetic dimers undergo a chemical bond and form a chemical dimer. The particles that form magnetic dimers in the beginning of the actuation phase are in contact for 20s with each other while the magnetic dimers that form at the end only have a very short interaction time. During the actuation phase the amount of dimers increases linearly. This means that the average time that they interact is half of the duration of the actuation phase. We now get

$$k_{agg}^{mag} = \frac{\Delta N_{chem}/N_{mag,tot}}{\frac{1}{2}t_{act}} \quad (3)$$

The maximum aggregation rate we can measure with this experimental setup is reached when all magnetic dimers are converted to chemical dimers, $\frac{\Delta N_{chem}}{N_{mag,tot}} = 1$. The measured aggregation rate in this case is $\frac{1}{\frac{1}{2}t_{act}}$ or in this project, 0.1 s^{-1}.

The lower limit of the aggregation rate is determined by error of the measurement. The spread during the measurement phases gives a mean and a standard deviation. If we plug the standard deviation in eqn. 3 we get the error in the aggregation rate. A typical error in this project is 0.01s^{-1}.

4 Experimental results

In this project several experiments were carried out in order to quantify the aggregation rate between antibody coated particles. In this chapter these experiments will be explained. In the first paragraph a selection is made between two bead types and steps of the functionalization protocol are tested. In paragraph 4.2 the suppression of non-specific binding with commonly used solutions is tested. In paragraph 4.3 the aggregation rate for specific interactions is obtained for a range of PSA concentrations. Also a control experiment is performed to ensure that the interactions are specific.

4.1 Particle aggregation during functionalization

Aggregation will be measured for magnetic particles. In this project we have investigated the use of silica particles (microParticles GmbH) and polystyrene particles (Ademtech). The beads have a coating of carboxyl groups before further functionalization. Ideally the particles have a low coefficient of variation in size. The size of the particle has influence on their magnetizability and consequently their aggregation rate. Particles with a large variation in size will have the large particles aggregate before small particles, which might give unreliable measurements. Another factor of influence is the aggregation during the functionalization. If the particles are in clusters before they get additional surface coatings their functionalization becomes inhomogeneous. Additionally, the dynamic range of the measurements becomes smaller because fewer monomers are available for dimer formation.

Electron microscope images in Fig 4.1a and Fig 4.1b show that silica particles are more monodisperse than polystyrene particles. This trait is in favour of silica particles however we still need to test the aggregation of both type of particles.

In order to determine the aggregation of the stock particles we measure the level of the |A4F| peak. The particle solutions with carboxyl coating were diluted to 1pM and sonicated before the measurement, which consists of just the first phase of the protocol described in chapter 3. The measurements are performed in MES and in PBS because the functionalization has been carried out in MES and the aggregation rate measurements are carried out in PBS. As seen in Fig. 4.1c a higher |A4f| peak is measured with Silica particles in both MES and PBS. This could be explained by higher levels of aggregation, or it could be attributed to a different contribution to the |A4f| component per dimer. To check if silica particles show higher levels of initial clustering, an actuation phase is applied to see if aggregation increases. We measure the dynamic range of the |A4f| peak to test if the silica particles indeed have higher aggregation. Fig. 4.1d shows that Ademtech particles show a larger increase of the amplitude of the |A4f| peak than the silica particles. This means that the silica particles show higher levels of aggregation in stock particles. A possible cause of this is that the silica particles have lower carboxyl surface concentration than the Ademtech particles (30 µmol/g vs 515 µmol/g). Carboxyl groups can dissociate the hydrogen leaving the particle with negative charge. With more carboxyl groups more negative charge can be built. Particles with the same charge repel each other. This effect is larger for Ademtech particles than for silica particles.

In spite of their high coefficient of variation in size, the Ademtech particles are still more desirable due to the lower aggregation during functionalization than the silica particles. The rest of the experiments is performed using Ademtech polystyrene particles.

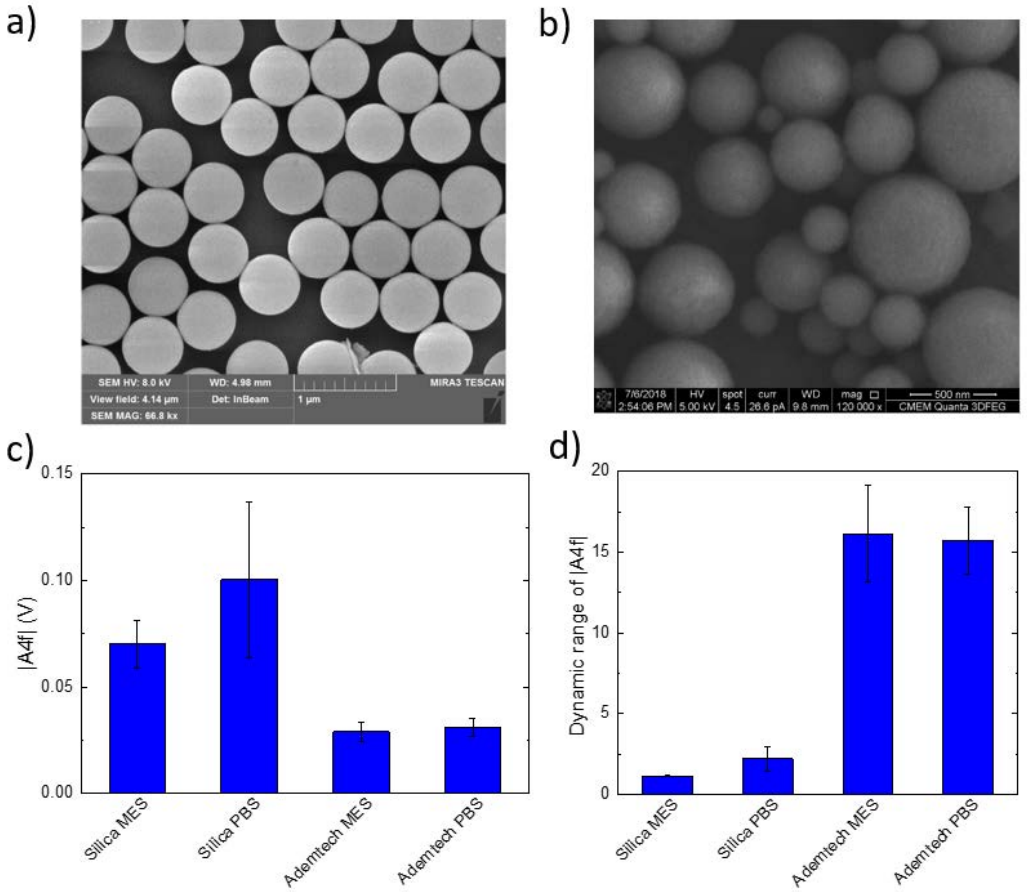

Fig. 4.1. Comparison between microParticles and Ademtech particles. *a) Electron microscope image of microParticles silica particles. b) Electron microscope image of Ademtech polystyrene particles. Images obtained from Max Scheepers. c) Background clustering for both particles with carboxyl coating during the first measurement phase of the measurement protocol. Measurements were done in PBS and MES. d) Dynamic range of particle aggregation for both particles measured with the first and second phase of the measurement protocol.*

To test which steps in the functionalization protocol cause clustering we follow the protocol described in chapter 3. In this protocol are three magnetic washing steps, each followed by a sonication step. The effect of this sonication step can be measured by eliminating the step at different points. Four samples are made and follow the functionalization protocol in parallel. Sample 1 skips all sonication steps, sample 2 only does the first sonication step, sample 3 does the first and second sonication step and sample 4 has all three sonication steps. Fig. 4.2 shows that only the protocol with all sonication steps has low background clustering. This indicates that magnetic washing causes aggregation of the particles. The sample with all sonication steps has low background clustering which indicates that this step breaks dimers apart. To test this, an extra sonication step is done after the measurement to each sample. This results in low background clustering for all samples.

Sonication step in protocol→	1	2	3
Sample 1			
Sample 2	✓		
Sample 3	✓	✓	
Sample 4	✓	✓	✓

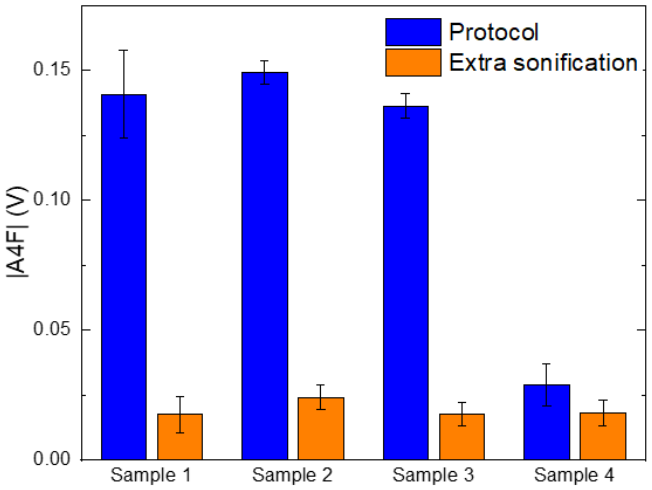

Fig. 4.2. Effect of sonication on aggregation during protocol. *Background clustering for four samples with increasing number of sonication steps. Another measurement was done after an extra sonication step.*

4.2 Suppression of non-specific interactions

To suppress the level of non-specific aggregation we have investigated three different substances that are commonly used to decrease particle aggregation. The particles are prepared according to the protocol of chapter 3, the last dilution step is done with a 10mg/ml solution of BSA, Tween-20 or pluronic F-127 in PBS. BSA is commonly used for its antifouling properties where it forms a corona around a particle that prevents aggregation of other molecules [10]. Tween-20 and pluronic F-127 are molecules that have ethylene chains that might sterically hinder the formation of dimers as was shown in the project of Stijn Haenen [6]. The exact function of these substances is beyond the scope of this project. The aggregation rate is measured for these samples according to the four step measurement protocol described in chapter 3. Fig. 4.3 shows that BSA has the lowest aggregation rate while Tween-20 and pluronic F-127 show no decrease in aggregation rate.

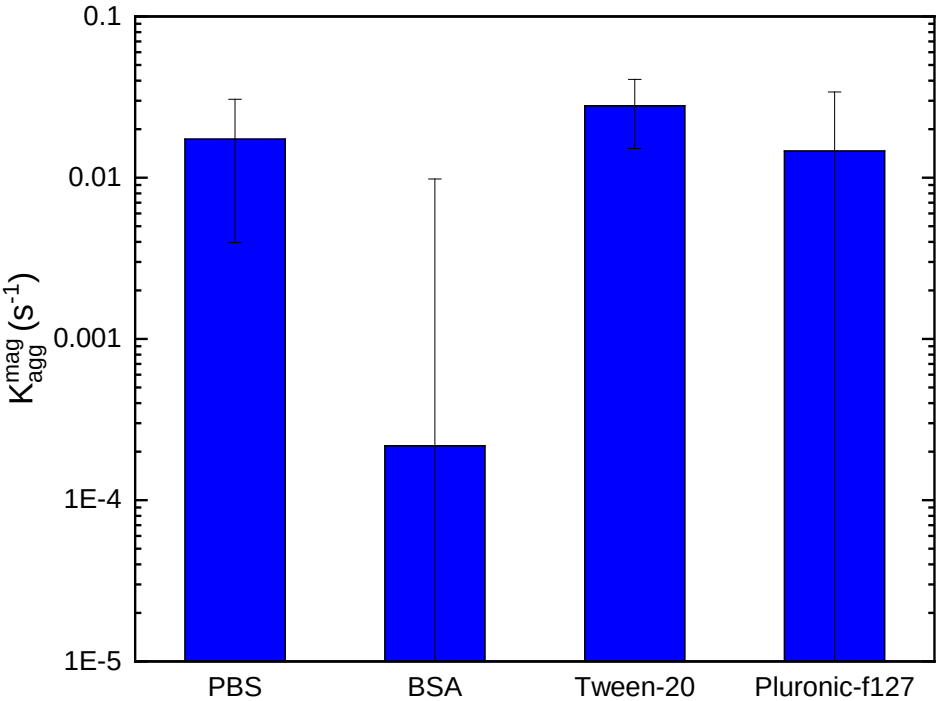

Fig. 4.3. Non-specific aggregation rates for aggregation suppressing substances. *Measurements of the aggregation rate for BSA, tween-20 and pluronic f-127 in PBS at a 10mg/ml concentration.*

4.3 Aggregation rate of specific interactions.

The goal of this project is to quantify the specific aggregation rate of antibody coated particles. In the following experiment we have functionalized particles with aPSA10 and particles with aPSA66. Before the measurement, PSA is added to the vial with aPSA10 particles and incubated for 5 minutes. After that, the aPSA10 particles and aPSA66 particles are mixed. The measurements are performed for a wide range of PSA concentrations. As a control that the aggregation is indeed specific, the same experiment is performed but with the same antibody types. This means that two antibodies cannot bind to the same PSA molecule and thus eliminating specific aggregation. Fig. 4.4 shows that the particles have increasing aggregation rate and reach the limit of the experimental setup of $0.1s^{-1}$. The samples of the control experiment do not show significant increase in aggregation rate, indicating that the aggregation between particles with different antibodies is specific. The dip in the high PSA concentration range could be caused by the excess of PSA molecules that block off all the antibodies on the aPSA66 particles during the experiment even though they did not have incubation time with the PSA molecules.

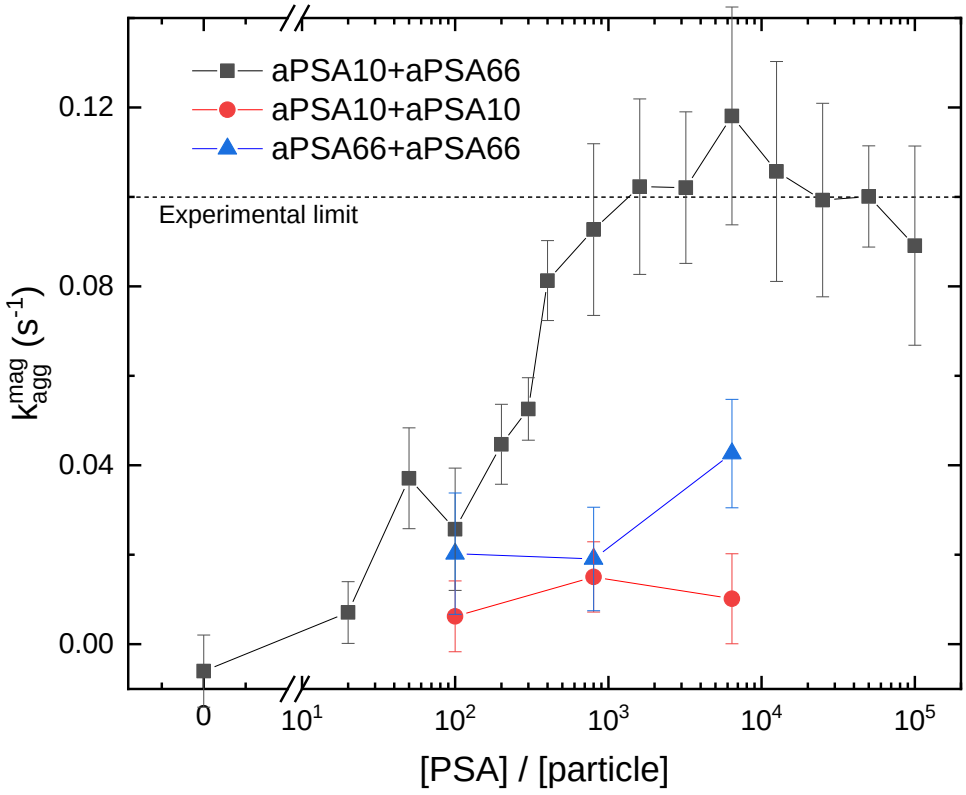

Fig. 4.4. Specific aggregation rate for particles with separate antibodies for varying PSA concentrations. *Measurement of particle aggregation rate where the particles have one type of antibody. The samples with the same type of antibody (red and blue) are a control experiment.*

To make a more direct comparison to the project of Stijn Haenen we also measured the aggregation rate for particles coated with both types of antibodies. The particles were functionalized with equal amounts of aPSA10 and aPSA66. PSA is added and incubated for five minutes before the measurement. For high PSA concentrations it is expected that the antibodies on the particles get saturated and cannot bind to a PSA molecule that is on another particle. Fig. 4.5 shows that the aggregation rate indeed decreases for high PSA concentrations. It is expected that if 50% of the available binding sites on the particles have captured a PSA molecule then the aggregation rate is highest. The experimental limit is reached so we cannot accurately locate the position of the peak.

To lower the aggregation rate we investigate the possibility of lowering antibody surface concentration from 6000 [ab]/[particle] during functionalization to 1778 [ab]/[particle] and 1185 [ab]/[particle]. Fig. 4.5 shows that the aggregation rate is indeed lowered and peaks can be discerned. For 1778 the peak is at around 4000 [PSA]/[particle] and for 1185 the peak is at around 2000 [PSA]/[particle]. The theoretical maximum number of available binding sites can be reached if all antibodies have gone onto the particle and all the antibodies are orientated so both of its paratopes are sticking outwards. In this case the amount of binding sites is two times the added [ab]/[particle] during functionalization. In practice however, the number of available sites is lower because the antibodies will not all bind to the particle and their orientation is more likely to be flat [11]. The amount of available PSA at the peaks is much higher than the 50% of available binding sites on the particle. This could be explained by the binding of PSA molecules to antibodies being slower than expected and needing a longer incubation time than 5 minutes. Longer incubation times however, have aggregation of the particles during the incubation as a result.

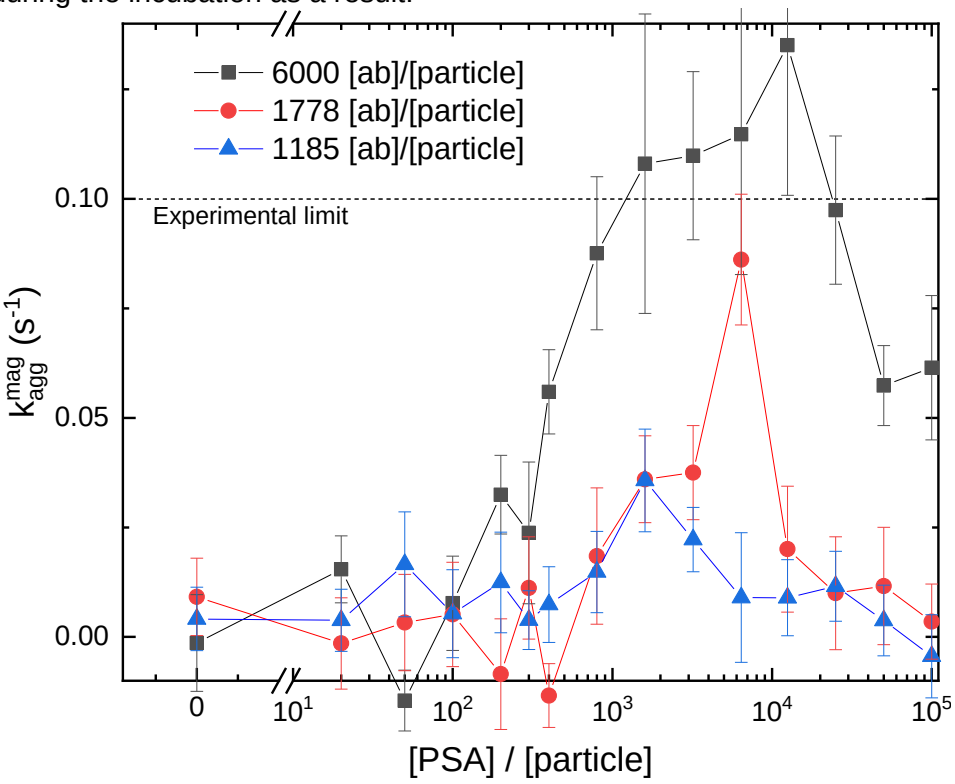

Fig. 4.5 Specific aggregation rate for particles with both types of antibodies in different surface concentrations. *Measurements of the specific aggregation rate for particles that have both aPSA10 and aPSA66 on their surface. For 6000 [ab]/[particle] the experimental limit is reached so lower surface of 1178 and 1185 [ab]/[particle] are measured also. The lines are obtained by taking the average of each point and its neighbors.*

5. Conclusion and outlook

In this project the specific aggregation rate was measured for PSA antibody coated particles using an optomagnetic cluster experiment. In order to do that we first investigated the properties of two particles, silica particles (microParticles GmbH) and polystyrene particles (Ademtech). It was determined that the aggregation in the silica particles was too high to use in this project. Most likely because of the lower surface concentration of carboxyl groups that can provide negative charge and create a repelling electrostatic force. We also investigated the potential causes of clustering during the functionalization process and determined that magnetically washing causes a lot of aggregation. The clusters can be broken apart with sonication.

We then investigated the use of three substances that are commonly used to prevent non-specific aggregation, BSA, Tween-20 and Pluronic F-127. It was found that only BSA gave a significant decrease in aggregation rate.

In order to quantify the specific aggregation rate we used particles that have only one type of antibody on their surface. We let the particles with one type of antibody incubate with PSA and later mix them with particles covered in the other type of antibody. The aggregation rate significantly increased with increasing concentration of PSA. As a control experiment we used only one type of particle during the experiment and this showed no increase in aggregation rate with increasing PSA concentration.

Lastly, to make a comparison to the project of Stijn Haenen, who made use of DNA docking strands and a complementary DNA analyte, we functionalized particles with both antibody types. This allowed for saturation of the binding sites and thus a decrease of aggregation rate at high PSA concentrations. We were able to tune the aggregation rate by decreasing the antibody surface concentration which allowed us to discern a peak that is below the experimental limit. The peak concentrations of PSA do not correspond to the theoretical values of available binding sites, possible due to slow binding of PSA to the antibody.

As a future experiment, longer incubation times of the PSA could be tested to see if the peak concentration matches more closely to the theoretical value. Another experiment that could be done is to try and tune the aggregation rate with PEG strands, like Stijn Haenen was able to do with the DNA system. Lastly, investigate if the aggregation rate of antibody coated particles could be measured in blood plasma instead of PBS to get closer to real diagnostics.

6. References

[1] Howes, P. D.; Chandrawatti, R.; Stevens, M. M. Colloidal nanoparticles as advanced biological sensors. *Science* **2014**, 346 (6205)

[2] Manuel Arruebo, Rodrigo Fernández-Pacheco, M. Ricardo Ibarra, Jesús Santamaría. Magnetic nanoparticles for drug delivery, Nano Today, Volume 2, Issue 3, **2007**, Pages 22-32

[3] Conroy Sun, Jerry S.H. Lee, Miqin Zhang. Magnetic nanoparticles in MR imaging and drug delivery. Advanced Drug Delivery Reviews, Volume 60, Issue 11, **2008**, Pages 1252-1265

[4] Baudry, J.; Rouzeau, C.; Goubault, C.; Robic, C.; CohenTannoudji, L.; Koenig, A.; Bertrand, E.; Bibette, J. Acceleration of the recognition rate between grafted ligands and receptors with magnetic forces. Proc. Natl. Acad. Sci. U.S.A **2006**, 103, 16076−16078.

[5] A. Ranzoni et al., One-step homogeneous magnetic nanoparticle immunoassay for biomarker detection directly in blood plasma, ACS Nano, **2012**, 6, 4, 3134-3141

[6] Stijn Haenen; Measuring and tuning specific particle aggregation rates using an optomagnetic cluster experiment, Master Thesis, Molecular Biosensing for Medical Diagnostiscs (MBX), Eindhoven University of Technology, **2019**

[7] Landry, J P et al. “Measuring affinity constants of 1450 monoclonal antibodies to peptide targets with a microarray-based label-free assay platform.” *Journal of immunological methods* vol. 417 (**2015**): 86-96. doi:10.1016/j.jim.2014.12.011

[8] J.C. Bacri, R. Perzynski, D. S. V. Cabuil, and R. Massart, “Magnetic colloidal properties of ionic ferrofluids,” J. Magnetism and Magnetic Materials, vol. 62, pp. 36–46, **1986**.

[9] van Vliembergen, R. W. L. *Optical scattering of rotating dimers for biosensing applications* Eindhoven: Technische Universiteit Eindhoven (**2018**).

[10] Qiang Peng et al. Preformed albumin corona, a protective coating for nanoparticles based drug delivery system. Biomaterials, Volume 34, Issue 33, **2013**, Pages 8521-8530, ISSN 0142-9612

[11] Bedabrata Saha. How Antibody Surface Coverage on Nanoparticles Determines the Activity and Kinetics of Antigen Capturing for Biosensing. Anal. Chem. (**2014**) 86, 16, 8158-8166